Surgical and Radiologic Anatomy (2019) 41:1369–1375
https://doi.org/10.1007/s00276-019-02342-4

ORIGINAL ARTICLE

Defining the shape of the scapulothoracic gliding surface

Tomas Paquet[1] · Robin Van Den Broecke[1] · Stijn Casier[1] · Jan Van Houcke[1] · Lieven De Wilde[1] · Alexander Van Tongel[1]

Received: 8 February 2019 / Accepted: 14 September 2019 / Published online: 15 October 2019

Abstract

Purpose The aim of the study is to evaluate the difference in shape of the upper part and lower part of the Scapulothoracic Gliding Surface (STGS).

Methods 3D-CT images of the thoracic cage of 50 patients were created in MIMICS ®. Three anatomical landmarks (insertion m. serratus anterior on 5th rib; transverse process of 2th and 7th vertebra) were used as an anteroposterior cutting plane to define the STGS. The upper part of the STG was defined as rib 2–5 and the lower part as 5–8. Next, in MATLAB ®, a script was used to create the sphere with best fit for upper and lower parts of STGS. The Root-Square-Mean Error (RSME) (mm) between two closest points on the fitted sphere and the STGS of both parts were calculated to determine the goodness-of-fit.

Results The RSME was found to be significantly lower for the area ribs 2–5 (mean 7.85 mm, SD 1.86) compared the area of ribs 5–8 (mean 10.08 mm, SD 1.90).

Conclusion The STGS of the upper thoracic wall (2–5) is more spherical shaped than the STGS of the lower thoracic wall (rib 5–8).

Keywords Anatomy · Ellipsoid · Thorax · Scapula · Motion

Introduction

The thoracic skeleton is an osseocartilaginous cage that protects the internal organs and has an important function in respiration. Expansion of the thorax, by contraction of the intercostal muscles and accessory muscles of respiration, results in ventilation of the lungs. However, the function of the thoracic cage is not only found in breathing. It also plays an eminent role in the movement of the upper limb.

Mobility of the shoulder originates from both motion in the glenohumeral joint as well as the kinematic interaction between scapula and thorax [13]. The role of the scapula is to provide proximal stability, acting as a base of support. It is an anchor attached to the thorax by 17 different muscles. Moving the scapula over the thorax allows for the glenoid to follow the movements of the humeral head. Thus, theoretically, the form of the thorax can have an influence on the thoracoscapular motion and accordingly on movement of the upper limb [15].

Literature described that in humans, the upper (ribs 1–5) and lower (ribs 6–10) thorax follows different ontogenetic trajectories [1]. Other research evaluated the morphological variations among adult population [11, 14]. Wang et al. described that thoracic size was primarily dominated by height and age–sex interaction, whereas shape was significantly dominated by age, sex, height, and BMI [14]. Xiangnan et al. narrated a geometric model, which shows significant effects on rib cross-section area for the parameters age, sex, and stature [11].

However, to our knowledge, no research has been done to evaluate the morphology of the thorax on which the scapulae moves and the difference between the upper part and the lower part of the thorax. This information may be helpful to create a biomechanical model that includes the shape of the thorax and to study the influence of thoracic morphology on scapular kinematics and the movement of the upper limb in humans.

The aim of this study is to describe the surface of the thorax on which the scapula glides in a normal population

Tomas Paquet and Robin Van Den Broecke Contributed Equally

✉ Tomas Paquet
Tomas_Paquet@hotmail.com

[1] Department of Orthopaedic Surgery and Traumatology, Ghent University Hospital, De Pintelaan 185, 9000 Ghent, Belgium

[defined as the scapulothoracic gliding surface (STGS)] and to evaluate the difference in shape between the upper and lower parts of the STGS.

Methods

This study was conducted from 17.3.2017 to 19.5.2018 with project numbers EC/2017/0230 and EC2017/032. Given approval by the UZ Gent Ethics Committee on 17.3.2017. The Belgian registration number is B670201731656. All patients signed an informed consent form.

In the Department of Nuclear Medicine at Ghent University Hospital, 64 patients undergoing a diagnostic PET-CT scan for any other reason than shoulder complaints were recruited. Patients were screened for shoulder pathology in their medical history with a short questionnaire. Patients with a history of shoulder pain or pathology were excluded from this study ($n=10$). During processing and evaluation of the CT images, patients with distinct deformities of the thoracic cage, e.g., caused by scoliosis, were excluded ($n=4$). Ultimately, 50 patients ($n=50$) were included in this study.

The raw data from the PET-CT-scan were reconstructed into slices with a thickness of 1.5 mm, taken at every 1 mm. Other technical CT parameters are: Convolution kernel: 170f, Pitch 0.7, Exposure time per rotation: 0.5 s, Peek kilovoltage: 120, Milliampere: 213. MIMICS® (version 18.0) was used to generate 3D images of the thoracic cage of the patients (Fig. 1).

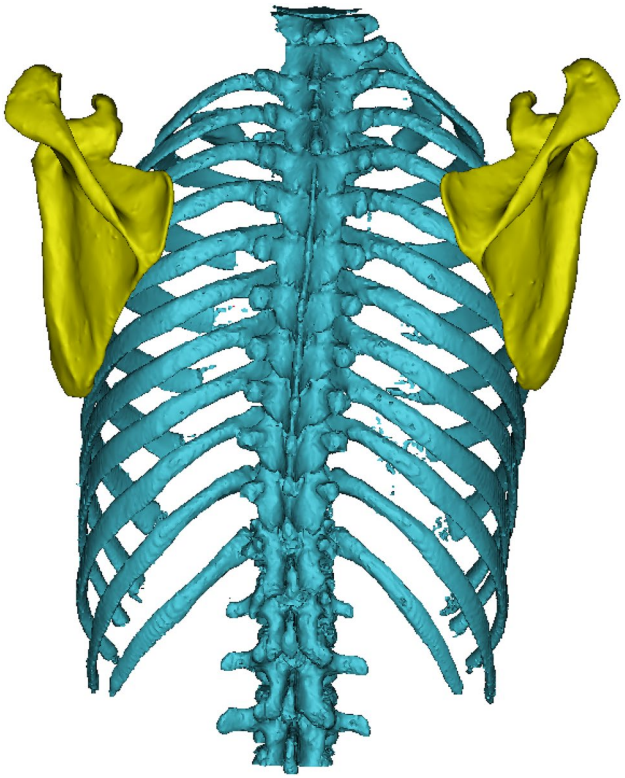

Fig. 1 Depiction of a 3D-image of a human thorax generated by MIMICS®. PET-CT-scan images were used to generate 3D images in MIMICS®

Reconstructing the scapulothoracic gliding plane

The scapula does not have contact with the whole surface of the thorax, but only moves over a limited part on the cranial side and posterior side (defined as the scapulothoracic gliding plane or surface). The goal of this study is to determine the shape of the thorax in relation to shoulder movement; therefore, only this relevant part of the thoracic cage was used for analysis. A new and reproducible method was created to define the relevant scapulothoracic gliding surface.

In MIMICS®, a plane was created, serving as a cutting plane to unilaterally separate the scapulothoracic gliding surface from the thoracic cage. This plane was defined by three points, assigned to anatomic landmarks, serving as the anteroposterior boundaries of the scapulothoracic surface (Fig. 2). These landmarks were:

- Insertion of the M. serratus anterior on the 5th rib.
- Most lateral tip of the transverse process of the 2nd thoracic vertebra.
- Most lateral tip of the transverse process of the 7th thoracic vertebra.

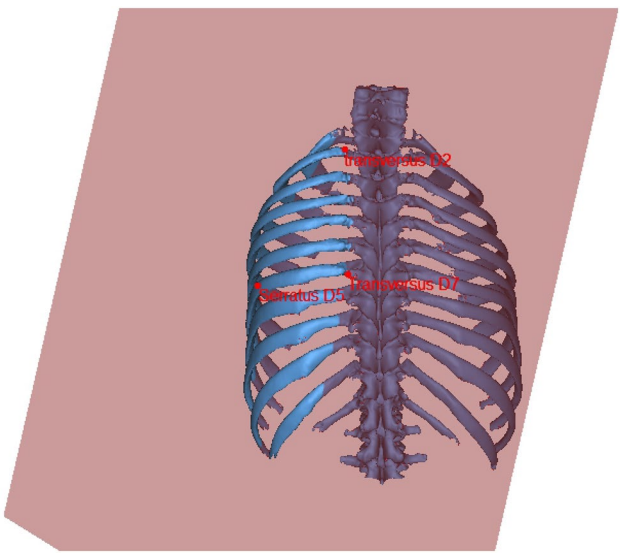

Fig. 2 Depiction of the scapulothoracic gliding surface cutting plane. Three anatomical points (insertion serratus 5th Rib, transverse process of D2, and transverse process of D7) were used to define the scapulothoracic gliding surface (STGS) cutting plane. This plane acted as the border of the STGS

The reasoning for these landmarks was that the movement of the scapula would respect the boundaries of the thoracoscapular muscles anteriorly (M. serratus anterior) and posteriorly (Mm. rhomboidei). The m. serratus anterior is the main protractor of the scapula; therefore, any protraction beyond its insertion is unlikely. Posteriorly, the interposition of the m. rhomboidei (retractor) and the paravertebral musculature prevents migration beyond the tip of the transverse process. Craniocaudally, the scapulothoracic gliding surface was defined to be between ribs two and eight. Therefore, only the area between these ribs was included.

The interclass (two researchers) and intraclass correlation coefficient (ICC, two-way random, absolute agreement), based on 20 measurements, was determined to evaluate the reproducibility of the chosen plane. An ICC larger than 0.70 was evaluated as good reproducibility.

Because only the shape of surface of the rib cage is relevant to the movements of the scapula, software program 3-MATICS® was used to generate a 3D image of the outer surface of the scapulothoracic gliding surface (Fig. 3).

Defining and fitting of an ellipsoid

In literature [2, 3, 5, 6, 10, 12], the thorax is usually represented by an ellipsoid. This study sets out to determine the dimensions and relative position of this ellipsoid representing the scapulothoracic gliding surface. A modified version of a MATLAB® script [8] was used to fit an ellipsoid to the scapulothoracic gliding surface, represented as a three-dimensional point cloud (Fig. 4).

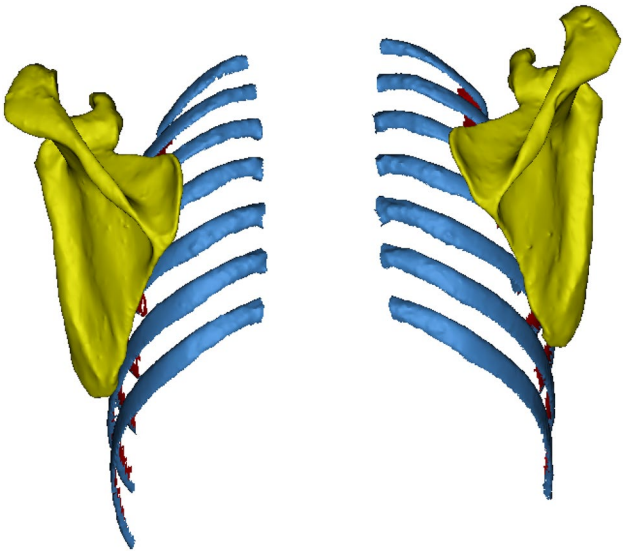

Fig. 3 Scapulothoracic gliding surface with scapulae. 3D depiction of the scapulothoracic gliding surface (STGS) as defined by the STGS cutting plane (blue) and scapulae (yellow) (color figure online)

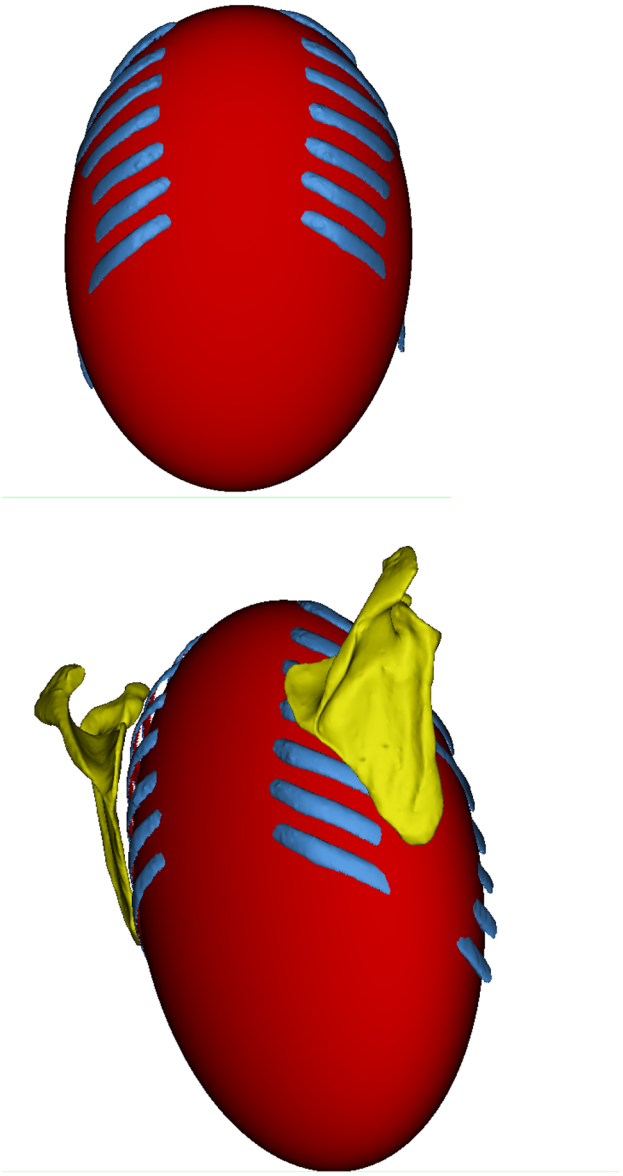

Fig. 4 Depiction of the scapulothoracic gliding surface ellipsoid. Ellipsoid (red) generated by MATHLAB® from bilateral STGS ribs 2–8 (color figure online)

Mathematically, an ellipsoid is derived from a sphere by directional scaling. It has 9° of freedom: three DOFs for the scaling (length of the three axes or the eigenvalues), three DOFs for the rotation, and three DOFs for the translation. It can be represented by the following equation with nine parameters (A–I):

$$Ax^2 + By^2 + Cz^2 + Dxy + Eyz + Fzx + Gx + Hy + Iz - 1 = 0.$$

To determine the rotation and translation, a coordinate system for the thorax was used, based on the ISB recommendations [16]. The origin of this coordinate system is coincident with the deepest point of the suprasternal notch (IJ).

The *Y*-axis is the line connecting the midpoint between the xiphoid (PX) process and the spinous process of T8 (T8) and the midpoint between the suprasternal notch and the spinous process of C7 (C7). The *Z*-axis is a line perpendicular to the plane formed by the suprasternal notch, the xiphoid process, and the spinous process of T8. The *X*-axis is the line perpendicular to the *Y*- and *Z*-axis. The *Y*-axis points upwards, the *Z*-axis points to the right, and the *X*-axis points forwards.

The center and axes of the ellipsoid were used to determine a coordinate system of the ellipsoid, with the center as origin, the length axis as *Y*-axis, the width axis as *Z*-axis, and the depth axis as *X*-axis. The translation was described by the distance between the center of the ellipsoid and the origin of the thoracic coordinate system. The rotations of the ellipsoid were described by Eulerian rotations in *Z*–*Y*–*X*-order.

To assess the goodness-of-fit between the fitted ellipsoid and the three-dimensional point cloud representing the STGS, the root-mean-square error (RMSE) of the distance in millimeters between every point of the STGS and the fitted ellipsoid was calculated.

Next, the upper and lower thoracic part of the STG was defined. As defined in the article of Bastir, rib 5 is used as the cutting point. To have an equal contribution of ribs at the upper and lower parts, the upper part is described by clustering rib 2–3–4 and 5 and the lower part by rib 5.6,7 and 8 (Fig. 5) [1].

To determine the goodness-of-fit of the ellipsoid to the STGS, the Root-mean-squared-error (RMSE) and standard deviation (STDEV) were calculated on the closest distances (in millimeters) from every point of the STGS to the closest point on the fitted ellipsoid for the full STGS and the upper and lower parts of the STGS.

To have a better understanding on the different form of ellipsoid, next, we used a fitted sphere to the upper and lower parts of the STGS. The smaller the RSME, the better it fits with a sphere, the larger the RSME, the better it fits with a cylinder. The percentiles of the RMSE were calculated in SPSS 24 to interpret the distribution and accuracy of the fitting procedure.

Results

In this study, 50 subjects were included, consisting of 30 male and 20 female subjects. The mean age was 55.4 years (std 15.7, min 20 year, max 78 year). Of the 50 subjects, 7 were left-handed and 43 right-handed.

We found excellent interobserver reliability for the scapulothoracic gliding plane with an ICC value of 0.91 (95% CI 0.83–0.95). With regards to the intraobserver reliability, we again found excellent intraobserver reliability with an ICC value of 0.92 (95% CI 0.84–0.96).

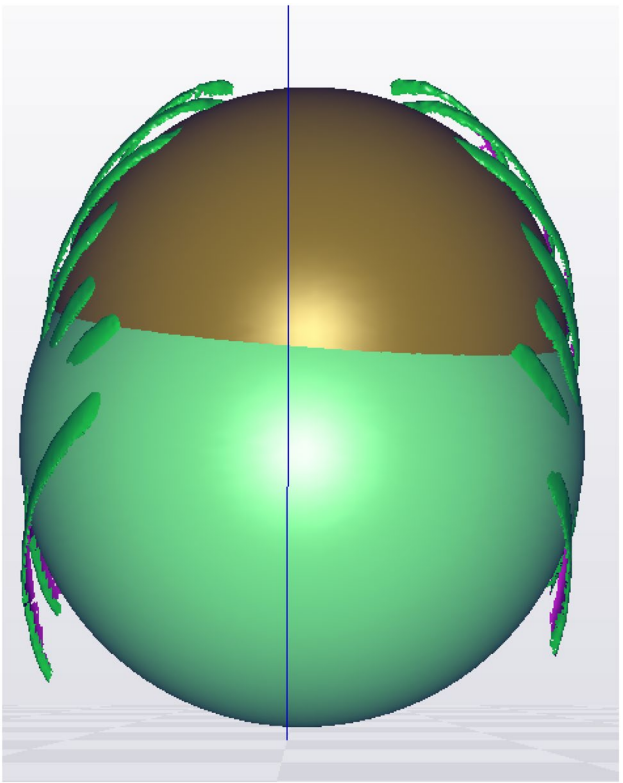

Fig. 5 Depiction of the scapulothoracic gliding surface sphere. Fitted spheres generated by MATHLAB® STGS rib 2–5 (gold) and STGS rib 5–8 (green) (color figure online)

Shape fitting of the complete bilateral STGSs.

In this section, the results of the shape fitting of a single ellipsoid into the STGSs bilaterally for the full surface (ribs 2–8) is described (Fig. 4). The goodness-of-fit was investigated by means of the RMSE. It is observed ellipsoids ($n = 50$) that 95% of the fitted have an RMSE between 3.23 and 6.62 (mm). Descriptive statistics are given in Table 1.

All three radii were found to be smaller in female compared to male patients ($p < 0.001$), but no significant difference in ratios (width–depth, width–height, and height–depth) were found.

Next, the ellipsoids were fitted into upper and lower parts of the STGS. Descriptive statistics for RSME for all clusters are given in Table 2. Using one-sample Kolmogorov–Smirnov test, normal distribution was observed for both clusters. Both clusters were paired to one another to observe RSME difference. Using two-tailed *t* test, significant RSME difference ($P < 0.05$) was shown in between clusters rib 2–5 (r25) and rib 5–8 (r58) ($P < 0.001$, paired sample correlation *t* test) (Fig. 6).

RSME between the both parts of the thoracic surface and fitted spheres was found to be significantly lower ($P < 0.001$, paired sample *t* test) for the area ribs 2–5 (RSME 25) (mean

Table 1 Descriptive statistics bilateral STGS ribs 2–8

($n=50$)	Minimum	Maximum	Mean	Std. deviation
RMSE	3.05	6.62	5.26	0.77
STDEV	1.88	4.38	3.23	0.49
Height/2	164.08	353.80	221.81	40.22
Width/2	118.14	168.32	143.55	13.62
Depth/2	62.57	137.47	100.51	15.02
X-coordinate (center)	− 103.61	− 20.59	− 52.61	15.41
Y-coordinate (center)	− 308.54	− 72.51	− 160.31	43.21
Z-coordinate (center)	− 17.29	16.22	1.63	5.42
Rotation *z*-axis	− 1.31	8.41	2.15	1.81
Rotation *y*-axis	0.98	52.80	10.57	7.28
Rotation *x*-axis	− 8.32	8.29	− 0.52	4.03
Height–width ratio	1.18	2.26	1.54	0.21
Height–depth ratio	1,8	3.00	2.22	0.27
Width–depth ratio	1.16	2.04	1.45	0.19

Table 2 Descriptive statistics of RSME of partial ellipsoids: rib 2–8, rib 2–5, and rib 5–8

	Minimum	Maximum	Mean	Std. deviation
r28	3.03	6.61	5.22	0.79
r25	2.52	7.20	4.94	1.02
r58	3.22	8.22	5.92	1.13

7.85 mm, SD 1.86) compared to the area of ribs 5–8 (RSME 58) (mean 10.08 mm, SD 1.90) (Fig. 7).

Discussion

The shape of the thorax is determined by biomechanical conditions. Maintaining body posture during the short alternating phases of locomotion demands larger muscle forces and imposes higher demands on the skeleton than free limb movements [9]. For this reason, an important explanation for the morphology of the thoracic skeleton can be found in locomotion. In cursorial animals (with an absent clavicle bone), the weight of head, neck, trunk, and abdomen is only supported by limb muscles. These are the M. serratus ventralis (M. serratus anterior in humans) and the M. pectoralis profundus (M. pectoralis minor). However, in this configuration, the ribs need to offer sufficient strength to withstand the large compressive forces caused by the muscles bearing the body weight, but remain mobile enough to allow for respiration. Evolutionary in these animals, a deep thoracic cage with flat ribs is seen, because this morphology is less prone to high bending forces. A different pattern is observed when abducting or elevating the shoulder joint [9]. These types of movements occur in primates during (arboreal) upper limb suspension and during reaching and grasping. Extreme passive abduction of the humerus is counteracted by M. pectoralis major. In elevation, the M. latissimus dorsi also plays an important role in shoulder joint stability. Furthermore, rotator cuff muscles work to pull the humeral head perpendicular to the glenoid. The resultant force is directed medially and dorsally [9].

From the standpoint of evolution, it would be natural that a structure is formed to support these forces. This support is in humans provided by the clavicle [13]. When a larger dorsal component of the force is present, the M. subclavius and M. pectoralis minor will prevent the scapula from moving too far dorsally. To withstand these medially directed forces, the ribs must be oriented along the force vectors. This means that the ribs have to be more mediolaterally oriented than in cursorial animals [9]. A shorter distance between rib attachment points (at sternum and spine) results in a smaller bending moment and higher axial rib compression, hence the strongly curved ribs that form a wide and shallow thorax [9].

As described in humans, the thorax can be divided based on a different ontogenetic trajectory within upper part (ribs 1–5) and lower part (ribs 6–10); likely, both with different function [1]. The upper part acts as an important a support for the shoulder girdle, whereas the lower part aids in respiration.

In this study, the morphology of thorax, specifically the gliding surface of the scapula, was examined. We did not include ribs 1, 9, and 10 in our measurement. To have an equal contribution of ribs, we described the upper part as rib 2–3–4 and 5 and the lower part as rib 5.6, 7, and 8. When fitting an ellipsoid, it was observed that the RSME is significant lower in upper part compared to the lower part.

Furthermore, there was a significant difference between the RSME of the upper and lower thorax STGS when fitting a sphere, indicating a more spherical shape of the upper STGS. This finding accompanies the hypothesis that the configuration of upper thoracic wall lends itself better for upper limb abduction and elevation than inferior thoracic anatomy. It could be proposed that the latter part provides a more adynamic protection of internal organs.

The knowledge of the different shapes of the thorax can be important when evaluating the scapulothoracic motion. Recent studies have highlighted an increased scapulothoracic contribution to achieve elevation in reversed- and total shoulder arthroplasty when compared to healthy subjects [4], proposing that the shape of upper STGS plays an important role in upper arm movement. It is possible that an increased importance could be observed for patients with reversed- or total arthroplasty when researched. Also, future studies

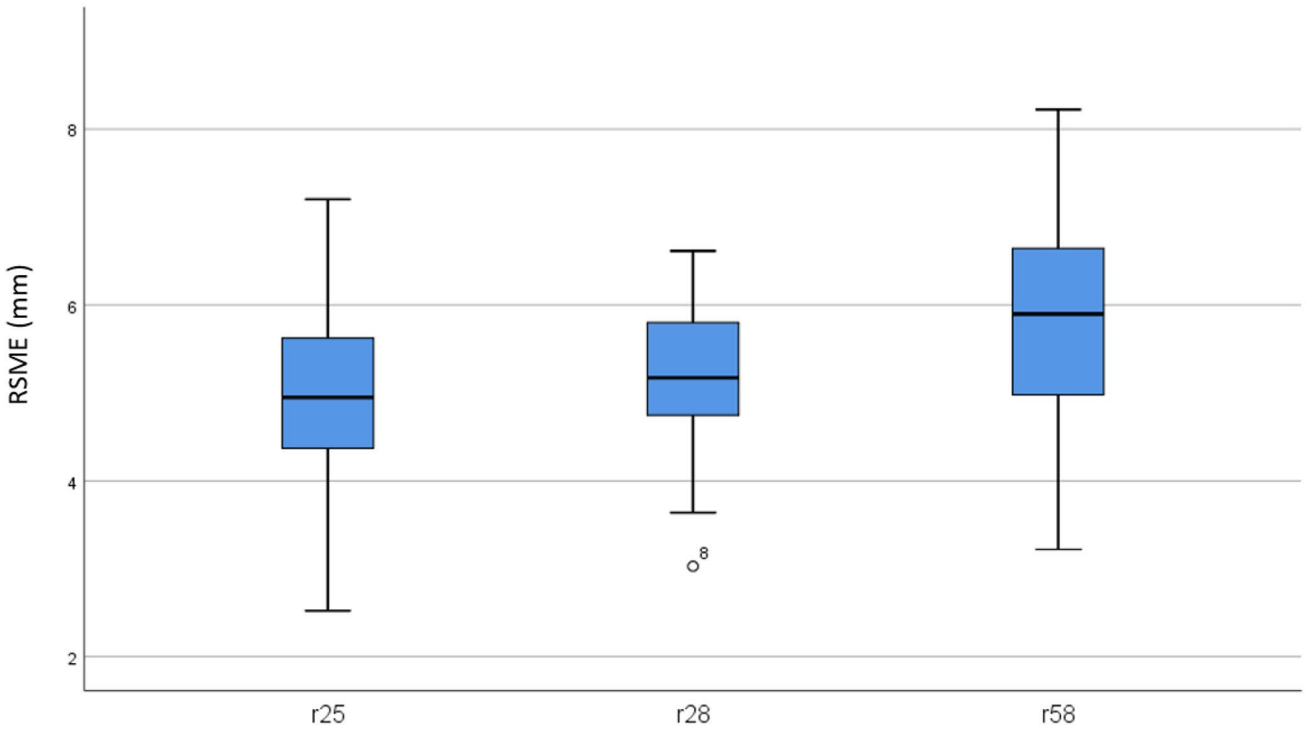

Fig. 6 RSME of ellipsoids created from partial STGS. Box- and Whiskers plot describing the RSME of partial ellipsoids created by clustering ribs 2–5 (r25), ribs 2–8 (r28), and ribs 5–8 (r58). Significant difference ($P < 0.001$, paired student T test) in between all clusters was observed. RSME of cluster rib 2–5 (upper thoracic wall) was found to be lowest, whereas the RSME of r85 was found to be highest. Significance difference ($P < 0.001$) in between all clusters was observed

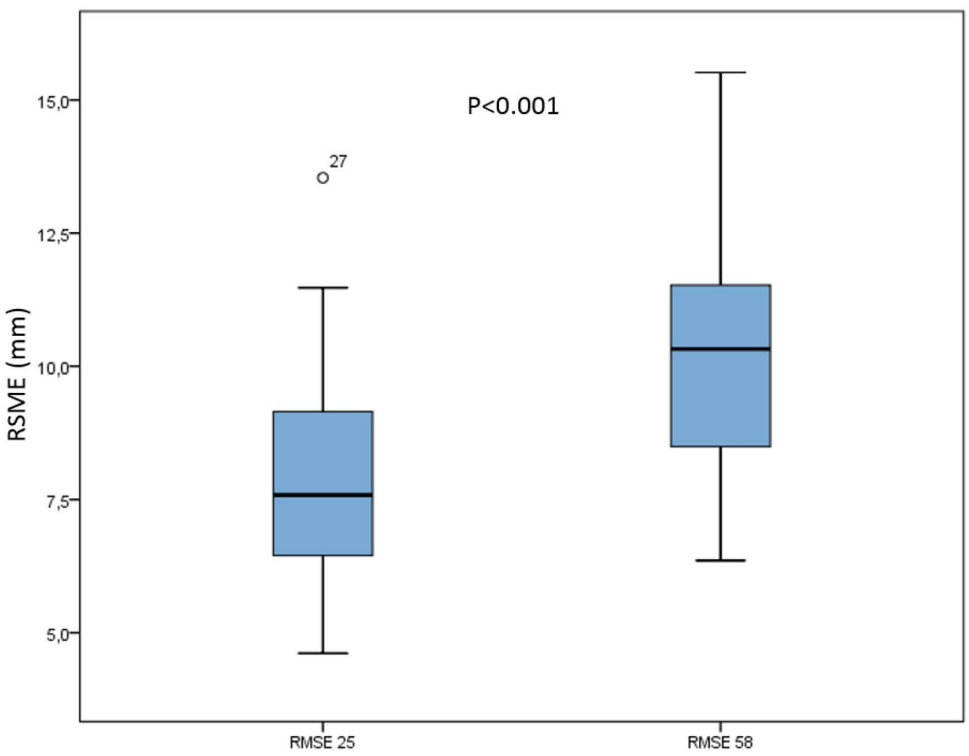

Fig. 7 RSME between the thoracic surface and fitted spheres created by clustering ribs 2–5 and ribs 5–8. Box and Whisker plot describing the RSME between the thoracic surface and fitted spheres created by clustering: rib 2–5 (RSME25) and ribs 5–8 (RSME58). RSME was found to be significantly lower ($P < 0.001$, paired sample t test) in the STGS of ribs 2–5 (upper thoracic wall) compared to STGS of ribs 5–8 (lower thoracic wall)

could evaluate the correlation of the scapulothoracic motion and the shape of the STGS to have a better understanding which variables that are static and which are dynamic.

In addition, it would be interesting to study whether or not a difference in STGS shape and its correlation between hypo- or hyperkyphosis contributes to different pathologies. It has already been described that individuals with hyperkyphosis have less thoracic spine extension and more scapular dyskinesia compared to those with healthy shoulders [7].

This research on basic STGS geometry can serve as a future reference for shoulder research and models. The final STGS would then to be described by combination of shapes, each with the potential to determine scapulothoracic movement over a different range. The next step is to evaluate the correlation between the shape of the scapula and the size of the ellipsoid in the normal population.

Conclusion

The upper part (rib 2–5) of the thoracic wall surface upon which scapula moves is representable with an ellipsoid. Also, we observed a significant difference between the morphology of the STGS of the upper and lower thoracic wall, indicating that the STGS of the upper thoracic wall (rib 2–5) is more spherical shaped than the STGS of the lower thoracic wall (rib 5–8).

Acknowledgements We want to thank Emmanuel Audenaert for his technical support.

Author contributions Casier: data collection. De Wilde: protocol/project development. Paquet: data collection and management, data analysis, manuscript writing, and editing. Van Den Broucke: data collection and management, data analysis, and manuscript writing. Van Houcke: data management. Van Tongel: protocol/project development and manuscript writing/editing.

Compliance with ethical standards

Conflict of interest No conflict of interest.

Informed consent Al participants were given informed consent.

Ethical approval All procedures performed in studies involving human participants were in accordance with the ethical standards of the institutional and/or national research committee and with the 1964 Helsinki declaration and its later amendments or comparable ethical standards.

References

1. Bastir M, Garcia Martinez D, Recheis W, Barash A, Coquerelle M, Rios L, Pena-Melian A, Garcia Rio F, O'Higgins P (2013) Differential growth and development of the upper and lower human thorax. PLoS One 8:e75128. https://doi.org/10.1371/journal.pone.0075128
2. Bolsterlee B, Veeger HE, van der Helm FC (2014) Modelling clavicular and scapular kinematics: from measurement to simulation. Med Biol Eng Comput 52:283–291. https://doi.org/10.1007/s11517-013-1065-2
3. Charlton IW (2003) A model for prediction of the forces at the glenohumeral join. Proc Inst Mech Eng [H] 220:801–812
4. De Toledo JM, Loss JF, Janssen TW, Van Der Scheer TW, Alta TD, Willems WJ, Veeger D (2012) Kinematic evaluation of patients with total and reverse shoulder arthroplasty during rehabilitation exercises with different loads. Clin Biomech 27:793–800. https://doi.org/10.1016/j.clinbiomech.2012.04.009
5. Der Helm FCT (1994) Analysis of the kinematic and dynamic behavior of the shoulder mechanism. J Biomech 27:527–550
6. Maurel W, Thalmann D (2000) Human upper limb modeling including scapulo-thoracic constraint and joint sinus cones. Comput Graph 24:203–218
7. Otoshi K, Takegami M, Sekiguchi M, Onishi Y, Yamazaki S, Otani K, Shishido H, Kikuchi S, Konno S (2014) Association between kyphosis and subacromial impingement syndrome: LOHAS study. J Shoulder Elbow Surg 23:e300–e307. https://doi.org/10.1016/j.jse.2014.04.010
8. Petrov Y (2009) Ellipsoid fit.The Mathworks Inc. https://www.mathworks.com/matlabcentral/fileexchange/24693-ellipsoid-fit. Accessed 1 Sept 2017
9. Preuschoft H, Schmidt M, Hayama S, Okada M (2003) The influence of three-dimensional movements of the forelimb on the shape of the thorax and its importance for erect body posture. Walk Upright 243:9–24
10. Seth A, Matias R, Veloso AP, Delp SL (2016) A biomechanical model of the scapulothoracic joint to accurately capture scapular kinematics during shoulder movements. PLoS One 11:e0141028. https://doi.org/10.1371/journal.pone.0141028
11. Shi X, Cao L, Reed MP, Rupp JD, Hoff CN, Hu J (2014) A statistical human rib cage geometry model accounting for variations by age, sex, stature and body mass index. J Biomech 47:2277–2285. https://doi.org/10.1016/j.jbiomech.2014.04.045
12. Van der Helm FC (1994) A finite element musculoskeletal model of the shoulder mechanism. J Biomech 27:551–569
13. Veeger HE, van der Helm FC (2007) Shoulder function: the perfect compromise between mobility and stability. J Biomech 40:2119–2129. https://doi.org/10.1016/j.jbiomech.2006.10.016
14. Wang Y, Cao L, Bai Z, Reed MP, Rupp JD, Hoff CN, Hu J (2016) A parametric ribcage geometry model accounting for variations among the adult population. J Biomech 49:2791–2798. https://doi.org/10.1016/j.jbiomech.2016.06.020
15. Wilk KE, Arrigo C (1993) Current concepts in the rehabilitation of the athletic shoulder. J Orthop Sports Phys Ther 18:365–378. https://doi.org/10.2519/jospt.1993.18.1.365
16. Wu G, van der Helm FCT, Veeger HEJ, Makhsous M, Van Roy P, Anglin C, Nagels J, Karduna AR, McQuade K, Wang XG, Werner FW, Buchholz B (2005) ISB recommendation on definitions of joint coordinate systems of various joints for the reporting of human joint motion—part II: shoulder, elbow, wrist and hand. J Biomech 38:981–992. https://doi.org/10.1016/j.jbiomech.2004.05.042